Supporting information of

Unlocking the potential of alkaline-earth metal active centers for nitrogen activation and ammonia synthesis: the role of s-d orbital synergy

Donghai Wu[1,2], Jiarui Wu[1], Haobo Li[1], Wenjing Lv[1], Yanhao Song[1], Dongwei Ma[1*], and Yu Jia[1*]

[1]Key Laboratory for Special Functional Materials of Ministry of Education, School of Materials Science and Engineering, Henan University, Kaifeng 475004, China

[2]Henan Key Laboratory of Nanocomposites and Applications, Institute of Nanostructured Functional Materials, Huanghe Science and Technology College, Zhengzhou 450006, China

[*]Corresponding author. E-mail: dwmachina@126.com (D. Ma).

[*]Corresponding author. E-mail: jiayu@henu.edu.cn (Y. Jia).

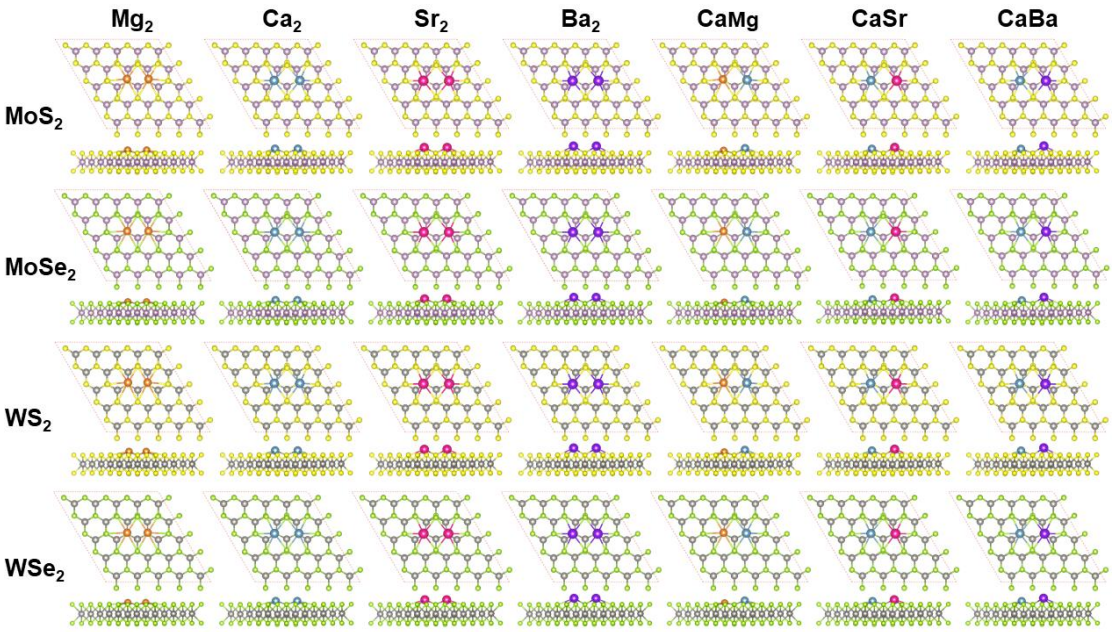

Fig. S1. Top and side views of the optimized configurations of AE_2@TMD DACs.

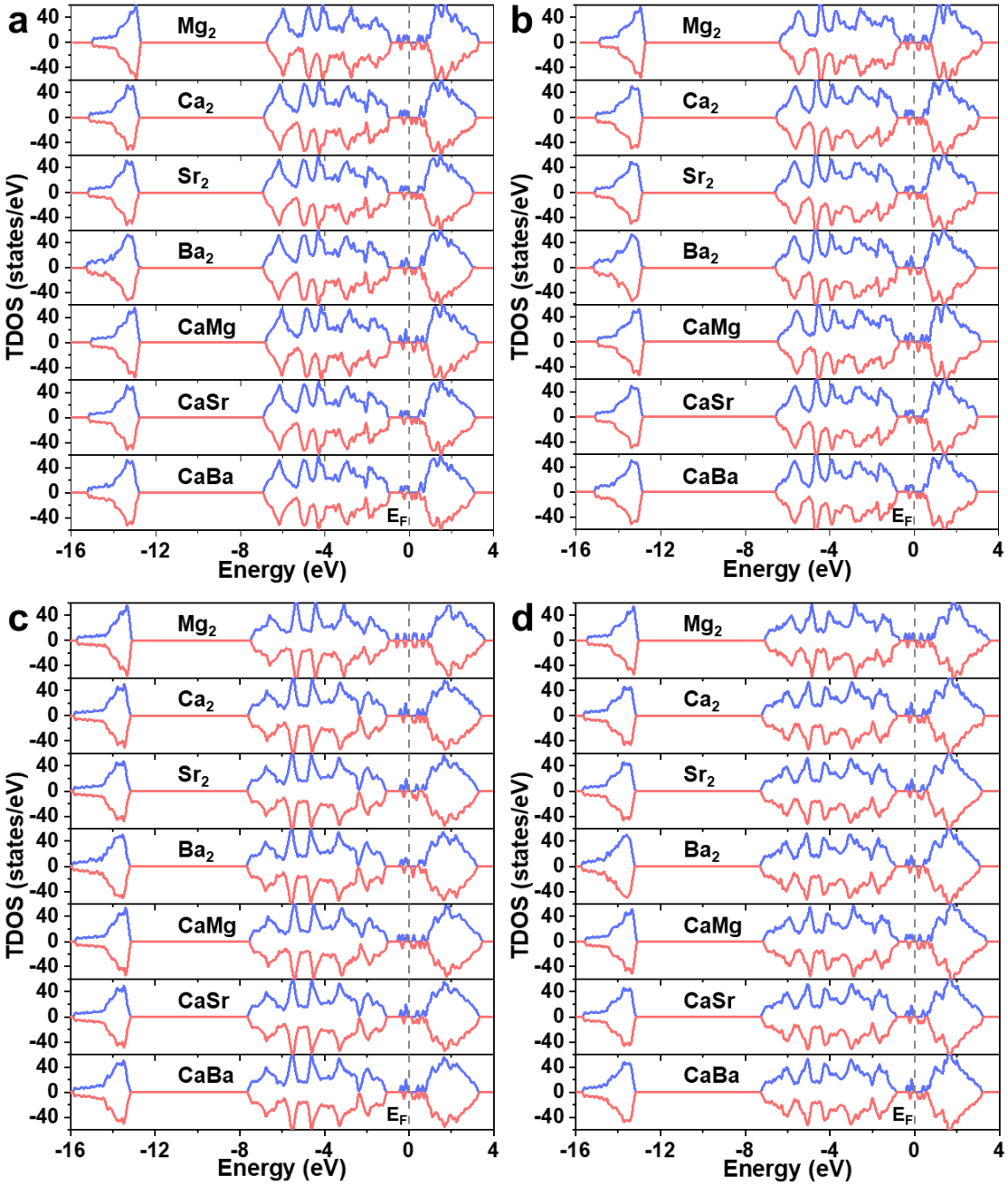

Fig. S2. Total DOS (TDOS) of the studied AE_2@TMD DACs supported by MoS_2 (a), $MoSe_2$ (b), WS_2 (c), and WSe_2 (d).

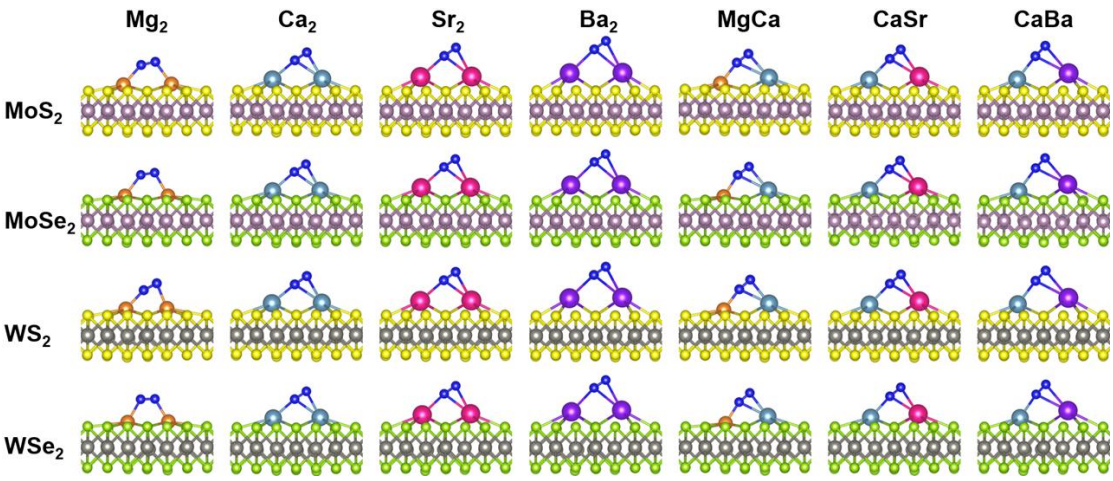

Fig. S3. The most favorable configurations of N_2 adsorption on the AE_2@TMD DACs.

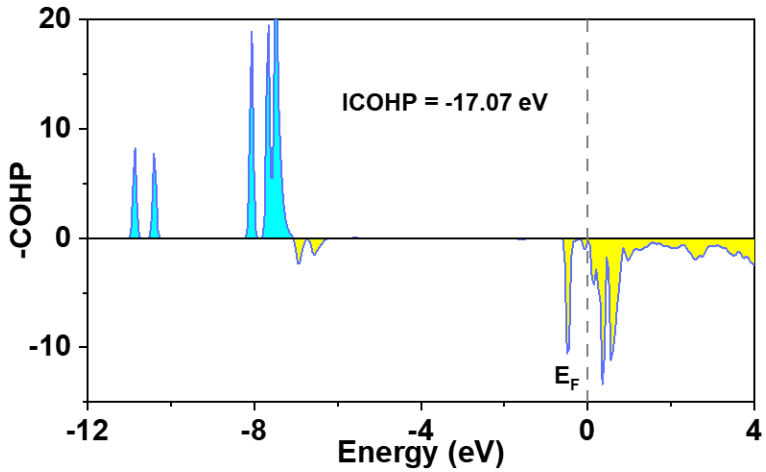

Fig. S4. Calculated COHP of $*N_2$ on $Ca_2@WS_2$ DAC. The vertical dashed line denotes the Fermi level, and the blue and yellow fills denote the bonding and antibonding interactions, respectively.

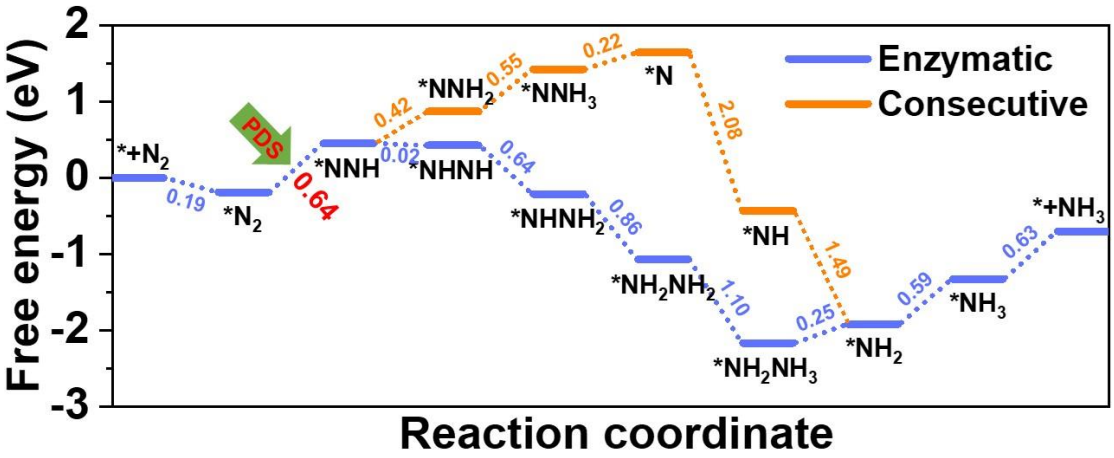

Fig. S5. Free energy diagram for NRR on CaBa@$MoSe_2$ DAC, with consideration of the solvation effect.

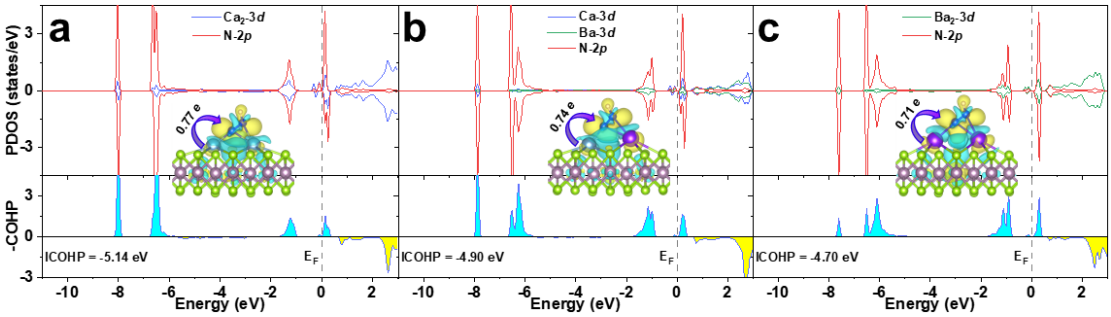

Fig. S6. PDOS of 3*d* orbitals of Ca/Ba and their bonded *N_2H, and the COHP between them for Ca_2@$MoSe_2$ (a), CaBa@$MoSe_2$ (b), and Ba_2@$MoSe_2$ (c). Insets are the corresponding CDD plots, where the yellow and cyan regions denote electron accumulation and depletion, respectively, with an isosurface of 0.001 *e*/bohr^3. The vertical dashed line in denotes the Fermi level. For the COHP, the blue and yellow fills denote the bonding and antibonding interactions, respectively.

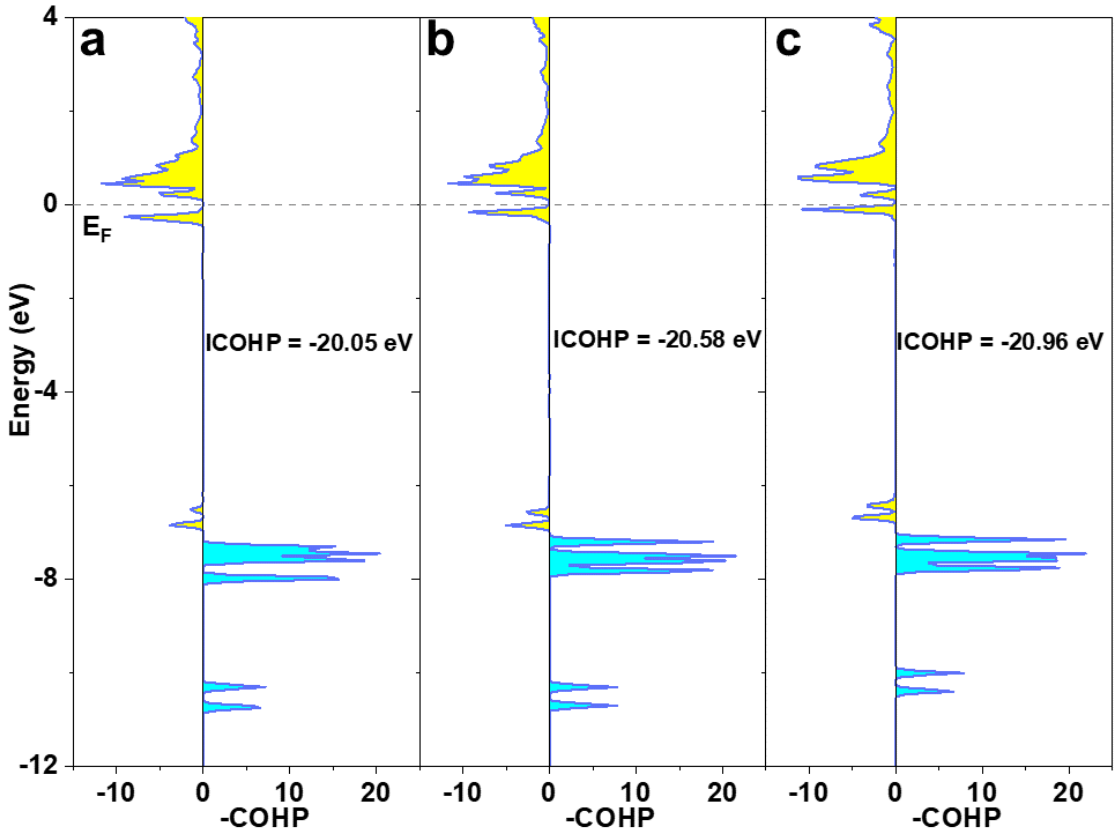

Fig. S7. Calculated COHP of $*N_2$ on Ca_2@$MoSe_2$ (a), CaBa@$MoSe_2$ (b), and Ba_2@$MoSe_2$ (c) DACs. The vertical dashed line denotes the Fermi level, and the blue and yellow fills denote the bonding and antibonding interactions, respectively.

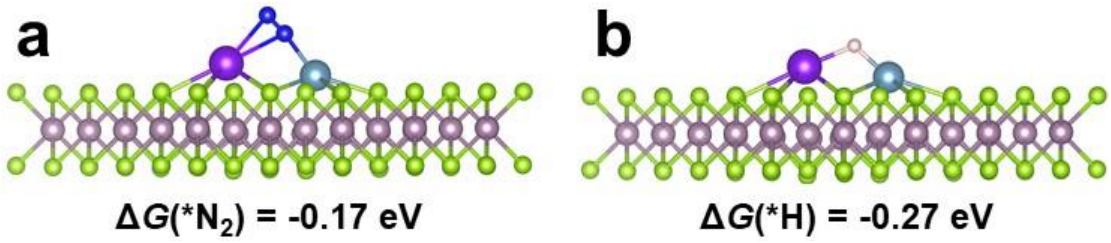

Fig. S8. The most favorable configurations of N_2 and H adsorption on the CaBa@$MoSe_2$ DAC together with the corresponding adsorption free energy.

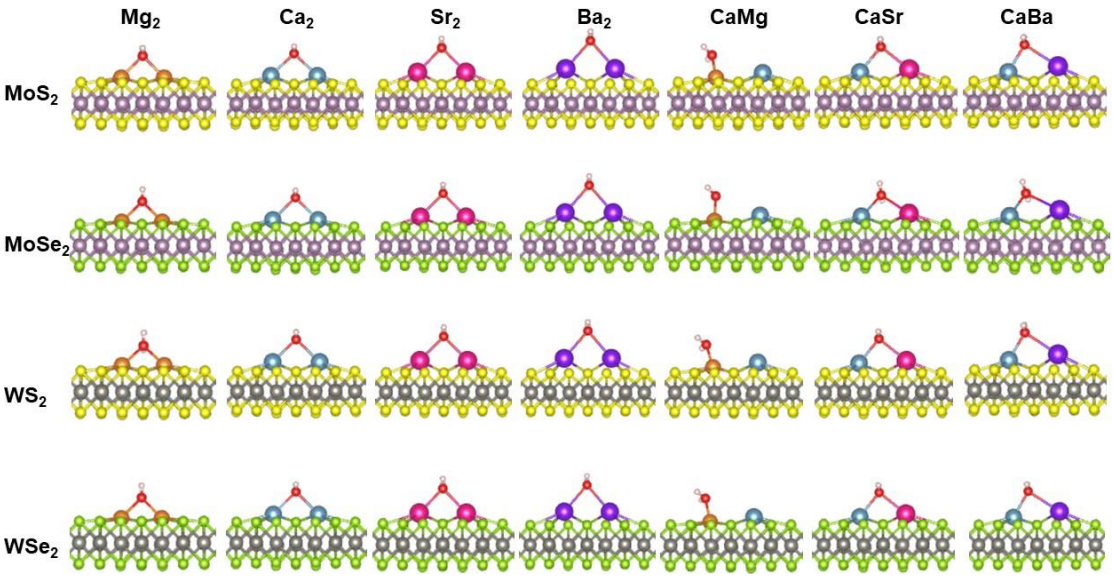

Fig. S9. The most stable configurations of H_2O adsorption on the AE_2@TMD DACs.

Table S1. Calculated zero-point energy (E_{ZPE}, in eV) and the product of temperature (T = 298.15 K) and entropy (S) (TS, in eV) of various species involved in the reaction pathways for NRR, where * represents the adsorption site.

Species	E_{ZPE}	TS
$*N_2$	0.18	0.15
*NNH	0.47	0.15
*NHNH	0.78	0.19
$*NHNH_2$	1.12	0.18
$*NH_2NH_2$	1.24	0.25
$*NH_2NH_3$	1.66	0.29
$*NNH_2$	0.81	0.15
$*NNH_3$	1.13	0.22
*N	0.08	0.03
*NH	0.31	0.10
$*NH_2$	0.66	0.10
$*NH_3$	1.00	0.22
N_2	0.15	0.58
H_2	0.27	0.41
NH_3	0.89	0.60

Table S2. Calculated dissolution potential (U_{diss}, in V) as well as N_2 and H_2O adsorption free energy ($\Delta G(*N_2)$, $\Delta G(*H_2O)$, in eV), N-N bond length of $*N_2$ ($d_{N\text{-}N}$, in Å), the number of the electron transferred from AE dimers to TMD support for pristine DACs (Q_{AE}, in *e*), and from the DACs to $*N_2$ on the studied AE_2@TMD DACs (Q_{*N2}, in *e*), where the positive and negative values represent losing and gaining electrons, respectively.

Systems	U_{diss}	$\Delta G(*N_2)$	$\Delta G(*H_2O)$	$d_{N\text{-}N}$	Q_{AE}	Q_{*N2}
Mg_2@MoS_2	-1.65	-0.13	-0.87	1.17	2.51	-0.65
Ca_2@MoS_2	-1.45	-0.32	-0.99	1.16	2.70	-0.59
Sr_2@MoS_2	-1.36	-0.24	-0.88	1.16	2.71	-0.57
Ba_2@MoS_2	-1.22	0.04	-0.66	1.15	2.56	-0.51
CaMg@MoS_2	-1.55	-0.30	-1.18	1.16	2.56	-0.57
CaSr@MoS_2	-1.40	-0.30	-0.95	1.16	2.71	-0.56
CaBa@MoS_2	-1.33	-0.23	-0.90	1.16	2.64	-0.52
Mg_2@$MoSe_2$	-1.62	-0.05	-0.94	1.17	2.55	-0.65
Ca_2@$MoSe_2$	-1.53	-0.23	-0.91	1.16	2.61	-0.59
Sr_2@$MoSe_2$	-1.47	-0.16	-0.81	1.16	2.61	-0.59
Ba_2@$MoSe_2$	-1.36	0.06	-0.61	1.16	2.44	-0.52
CaMg@$MoSe_2$	-1.57	-0.22	-1.11	1.16	2.58	-0.57
CaSr@$MoSe_2$	-1.50	-0.21	-1.00	1.16	2.62	-0.58
CaBa@$MoSe_2$	-1.44	-0.17	-0.98	1.16	2.54	-0.53
Mg_2@WS_2	-1.86	-0.09	-0.73	1.18	2.36	-0.74
Ca_2@WS_2	-1.75	-0.47	-0.97	1.17	2.64	-0.61
Sr_2@WS_2	-1.68	-0.36	-0.85	1.16	2.65	-0.61
Ba_2@WS_2	-1.52	-0.05	-0.63	1.16	2.48	-0.53
CaMg@WS_2	-1.82	-0.37	-1.11	1.17	2.45	-0.66
CaSr@WS_2	-1.71	-0.44	-0.93	1.16	2.64	-0.61
CaBa@WS_2	-1.63	-0.35	-0.88	1.16	2.57	-0.56
Mg_2@WSe_2	-1.86	-0.19	-0.86	1.18	2.52	-0.74
Ca_2@WSe_2	-1.82	-0.37	-0.90	1.17	2.56	-0.63
Sr_2@WSe_2	-1.77	-0.31	-0.79	1.17	2.55	-0.64
Ba_2@WSe_2	-1.64	-0.04	-0.58	1.16	2.37	-0.56
CaMg@WSe_2	-1.84	-0.36	-1.08	1.17	2.50	-0.68
CaSr@WSe_2	-1.80	-0.35	-0.86	1.17	2.56	-0.62
CaBa@WSe_2	-1.73	-0.32	-0.82	1.16	2.47	-0.58

Table S3. Calculated limiting potential (U_L, in V), potential-determining step (PDS), and reaction free energy of the first hydrogenation ($*N_2 + H^+ + e \rightarrow *N_2H$) ($\Delta G_1$, in eV) and last hydrogenation ($*NH_2 + H^+ + e \rightarrow *NH_3$) ($\Delta G_6$, in eV) for NRR on the studied AE_2@TMD DACs.

Systems	U_L	PDS	ΔG_1	ΔG_6
Mg_2@MoS_2	-0.93	$*NH_2 \rightarrow *NH_3$	0.42	0.93
Ca_2@MoS_2	-0.97	$*NH_2 \rightarrow *NH_3$	0.45	0.97
Sr_2@MoS_2	-0.97	$*NH_2 \rightarrow *NH_3$	0.55	0.97
Ba_2@MoS_2	-0.71	$*N_2 \rightarrow *N_2H$	0.71	0.68
CaMg@MoS_2	-0.83	$*NH_2 \rightarrow *NH_3$	0.39	0.83
CaSr@MoS_2	-0.92	$*NH_2 \rightarrow *NH_3$	0.53	0.92
CaBa@MoS_2	-0.75	$*NH_2 \rightarrow *NH_3$	0.61	0.75
Mg_2@$MoSe_2$	-0.78	$*NH_2 \rightarrow *NH_3$	0.39	0.78
Ca_2@$MoSe_2$	-0.77	$*NH_2 \rightarrow *NH_3$	0.46	0.77
Sr_2@$MoSe_2$	-0.79	$*NH_2 \rightarrow *NH_3$	0.54	0.79
Ba_2@$MoSe_2$	-0.67	$*N_2 \rightarrow *N_2H$	0.67	0.46
CaMg@$MoSe_2$	-0.70	$*NH_2 \rightarrow *NH_3$	0.38	0.70
CaSr@$MoSe_2$	-0.70	$*NH_2 \rightarrow *NH_3$	0.52	0.70
CaBa@$MoSe_2$	-0.60	$*N_2 \rightarrow *N_2H$	0.60	0.56
Mg_2@WS_2	-0.86	$*NH_2 \rightarrow *NH_3$	0.37	0.86
Ca_2@WS_2	-1.13	$*NH_2 \rightarrow *NH_3$	0.37	1.13
Sr_2@WS_2	-1.10	$*NH_2 \rightarrow *NH_3$	0.51	1.10
Ba_2@WS_2	-0.66	$*N_2 \rightarrow *N_2H$	0.66	0.61
CaMg@WS_2	-0.91	$*NH_2 \rightarrow *NH_3$	0.24	0.91
CaSr@WS_2	-1.05	$*NH_2 \rightarrow *NH_3$	0.46	1.05
CaBa@WS_2	-0.87	$*NH_2 \rightarrow *NH_3$	0.56	0.87
Mg_2@WSe_2	-1.06	$*NH_2 \rightarrow *NH_3$	0.38	1.06
Ca_2@WSe_2	-1.09	$*NH_2 \rightarrow *NH_3$	0.39	1.09
Sr_2@WSe_2	-1.04	$*NH_2 \rightarrow *NH_3$	0.53	1.04
Ba_2@WSe_2	-0.80	$*N_2 \rightarrow *N_2H$	0.80	0.67
CaMg@WSe_2	-1.02	$*NH_2 \rightarrow *NH_3$	0.28	1.02
CaSr@WSe_2	-1.03	$*NH_2 \rightarrow *NH_3$	0.47	1.03
CaBa@WSe_2	-0.87	$*NH_2 \rightarrow *NH_3$	0.62	0.87